Contributions in Science, 521:1–12 2 April 2013

Indications of Periodontal Disease in a Fossil Odontoceti (Mammalia: Cetacea) from the Late Miocene Monterey Formation at San Clemente Island, Southern California[1]

Sheila S. Flynn,[2] Randolph J. Moses,[2,3] and Jon H. Connolly[2]

ABSTRACT. An incomplete skull of a fossil odontocete from the Monterey Formation of late Miocene age on San Clemente Island, California, USA, includes an incomplete rostrum with an associated tooth. Below its cementoenamel junction, the tooth has a mineral deposit encircling the tooth that thickens apically into a bulge. On the root side of the bulge the deposit becomes thin with a stippled texture. The encircling mineral deposit corresponds anatomically to the gingival line and the circumference of the alveolus. The mineral deposit displays characteristics consistent with dental calculus, an indication of localized periodontal disease, and is believed to be the first documented occurrence of periodontal disease and calculus in a fossil cetacean.

INTRODUCTION

Paleopathology, the field that investigates how disease processes are manifest in the fossil record, shows that pathologies of fossil specimens are directly comparable to those evident in living species (Gerholdt and Godfrey, 2010; Rothschild and Martin, 2006, 1993; Moodie, 1923). Periodontal disease exists in fossil mammals and extant mammals (Hart Hansen et al., 1991; Dobney and Brothwell, 1988, 1986; Page and Schroeder, 1982; Bjotvedt and Turner, 1977) and periodontal disease in extant dolphins has been reported from the eastern South Pacific (Van Bressem et al., 2006, 2007). However, periodontal disease in fossil odontocetes has not been documented in the literature.

Dental plaque, a biofilm, coats teeth and can later become dental calculus (Cobb, 2008; Abraham et al., 2007; Hillson, 2005; Carranza and Newman, 1995). The cell walls of bacteria serve as a nucleus for calcium phosphate precipitation (Hillson, 2005). In addition to the surface biofilm, viable periodontal pathogens have been identified within the calculus matrix. Microbial biofilm is the primary cause of periodontal disease, with calculus being secondary because it acts as a reservoir for bacteria (Cobb, 2008; Socransky and Haffajee, 2005).

Calculus on the root of a tooth confirms the presence of long-standing plaque deposits and the presence of pathogenic bacteria that resulted in the destruction of the soft tissues, including gingiva and periodontal ligaments, and of bone. Thus calculus indicates periodontal disease (Cobb, 2008; Hillson, 2005; Carranza and Newman, 1995). Periodontitis includes a variety of bacterial diseases that, through inflammation, cause destruction to the periodontium (Craig et al., 2007; Gurenlian, 2007; Overman, 2006; Socransky and Haffajee, 2005; Socransky, 1970) (Fig. 1). Teeth can eventually fall out when the bone level and soft tissue attachment can no longer support teeth (Cobb, 2008; Craig et al., 2007; Hillson, 2005; Carranza and Newman, 1995).

Rohanizadeh and LeGeros (2004) utilized scanning electron microscopy (SEM), transmission electron microscopy, and Fourier-transform infrared spectroscopy to identify the characteristics of calculus. Macroscopically, dental calculus appears irregular, coarse, and coated with microbial biofilm (plaque) (Cobb, 2008; Tan et al., 2004; Lustmann et al., 1976; Fig. 2 herein). Compared to enamel, supragingival calculus is loosely structured with significant porosity and permeability. Forsberg et al. (1960) studied microradiographic images of supragingival calculus and reported stratified layers near the surface of the calculus. In some cases the calculus was more homogeneous near the tooth surface. Calculus that forms subgingivally can be homogeneous and uniform, being compressed by gingival tissues (Lustmann et al., 1976), and exhibits a similar pattern to the enamel–calculus interface (Rohanizadeh and LeGeros, 2004). Fracture planes occur within the calculus near, but not at, the calculus–enamel interface and not within the calculocementum and are due to the higher level of microporosity within the calculus than the bonding at the calculus–tooth interface (Abraham et al., 2007; Rohanizadeh and LeGeros, 2004) (Figs. 2A, 2B). The gingival line can recede toward the root tip, exposing the cementum covering the root. Recession of the gingiva can be caused by periodontal infections, soft tissue trauma, and super-eruption caused by an unopposed tooth (Hillson, 2005; Carranza and Newman, 1995).

Extant Odontoceti, like humans, are subject to periodontal disease. Twenty percent of the mature long-beaked common dolphins (*Delphinus capensis* Gray, 1828) studied from the eastern South Pacific possessed lesions of the alveoli. Lesions of the alveoli, an indication of periodontal disease, are commonly caused by bacterial infections (Van Bressem et al. 2006). Periodontal disease has also been documented in other extant odontocete cetaceans, including the bottlenose dolphin (*Tursiops truncatus* [Montagu, 1821]), dusky dolphin (*Lagenorhynchus obscurus* [Gray, 1828]), short finned pilot whale (*Globicephala macrorhynchus* Gray, 1846), long finned pilot whale (*G. melas* [Traill, 1809]), Risso's dolphin (*Grampus griseus* [G. Cuvier, 1812]), and Burmeister's porpoise (*P. spinipinnis* Burmeister, 1865) (Perrin, 2010) (Van Bressem et al., 2007, 2006).

The purpose of this paper is to describe and to identify a mineral deposit found on the fossil odontocete tooth (Fig. 3). This deposit shows characteristics that are consistent with dental calculus found in extant cetaceans and humans.

MATERIAL AND METHODS

In 2004 a partial odontocete skull (Sheridan College Museum of Geology [SCMG] 0665) was discovered in the Miocene Monterey Formation at

[1] URL: www.nhm.org/scholarlypublications

[2] Sheridan College Museum of Discovery, 3059 Coffeen Avenue, Sheridan, Wyoming 82801, USA. E-mail: sheilardh@bresnan.net

[3] Museum of Geology, South Dakota School of Mines and Technology, 501 East Saint Joseph Street, Rapid City, South Dakota 57701, USA.

© Natural History Museum of Los Angeles County, 2013
ISSN 0459-8113 (Print); 2165-1868 (Online)

Table 1 From EDX spectrum report on the mineral deposit of SCMG 0665 (Fig. 7) Elemental composition is consistent with calcium phosphate (hydroxyapatite).

Element	Wt (%)	At (%)
C	17.60	34.00
O	17.92	25.99
Na	0.06	0.06
Mg	0.28	0.26
Al	0.00	0.00
Si	0.53	0.44
P	14.00	10.49
S	0.66	0.48
Ca	48.55	28.11
Mn	0.36	0.15
Fe	0.00	0.00
Ti	0.00	0.00
K	0.04	0.02
Total	100.00	100.00

Abbreviations: At = Atomic; Wt = Weight

Table 2 From EDX spectrum report for the area analyzed (Fig. 9), indicated by a cross mark on the microbial tubule. Elemental composition is consistent with calcium carbonate.

Element	Wt (%)	At (%)
C	15.42	25.13
O	42.03	51.41
Na	0.66	0.56
Mg	1.96	1.58
Al	0.84	0.61
Si	4.62	3.22
P	5.84	3.69
S	0.46	0.28
Ca	26.18	12.78
Mn	0.05	0.02
Fe	1.62	0.57
Ti	0.07	0.03
K	0.23	0.11
Total	100.00	100.00

Abbreviations: At = Atomic; Wt = Weight

Horse Beach Canyon, on San Clemente Island, California, by one of us, (S.S.F.). Elements recovered include the rostrum, a petrosal, and a partial tooth root in one alveolus. An additional tooth found associated with the partial skull is the subject of this study.

San Clemente Island is a naval base and Horse Beach Canyon is a training area with severely limited access. Only two partial days were granted for exploration in 2004 and 2005 at Horse Beach Canyon. The cranium and rostrum were collected in the field, photographed in situ, then transported to the nearby Natural Resource Office lab on the island. During preparation the tooth was found in the sediments surrounding the cranium. Dental calculus was noted on the tooth upon inspection with a microscope. The tooth, cranium, and rostrum are currently conserved at Sheridan College.

The image of a male *Pontoporia blainvillei* (Gervais and d'Orbigny, 1844) tooth, Natural History Museum of Los Angeles County (LACM) 47143 from Punta del Diablo, Uruguay, was provided by the Mammalogy Department of the LACM. The LACM Vertebrate Paleontology Department provided an image of the tooth of an undescribed species of allodelphinid plantanistoid odontocete from the early Miocene Nye Formation in Oregon (LACM 123887).

SEM was used to evaluate the mineral deposit on the tooth from SCMG 0665. The tooth was carbon-coated under vacuum and analyzed using a Zeiss Supra40VP, variable-pressure, field-emission SEM with energy-dispersion X-ray capabilities (EDX), operating with acceleration voltage of 10–20 kV. SEM images were taken on several surfaces, including enamel, root, cementoenamel junction (CEJ), pulp cavity, and a chipped area of the bulge encircling the root.

RESULTS

The tooth associated with cranium SCMG 0665 lacks its crown tip and root and fits into the alveoli of the maxilla. However, its precise position in the tooth row cannot be assessed. A mineral deposit that encircles the tooth below the CEJ producing a bulge (Figs. 3, 4). The tooth is curved lingually with a white deposit that follows the longitudinal aspect of the tooth. In buccal view, the tooth exhibits a distinctly shiny enamel surface with longitudinal craze lines. The mineral deposit on the root surface displays a stippled pattern. The lingual view reveals the apical foramen and pulp canal in the crown.

On the lingual side of the tooth below the CEJ there is a chip in the circular bulge (Fig. 4). Under increased magnification, microbial tubules can be observed (Figs. 4, 5B, 6, 7, 9). In Figure 9, the marked tubule measures approximately 22 μm long × 7 μm wide. In comparison, a hyphae of *Actinomycetes,* a bacterium found in a human oral cavity, can measure 20 μm or longer with a width of 0.5–2.0 μm (Prescott et al., 1990).

EDX analyses were completed on tooth surfaces and microbial tubules (Figs. 7–10; Tables 1, 2). Rohanizadeh and LeGeros (2004) reported that calculus away from the tooth surface is heterogeneous because of the spaces once occupied by microorganisms and the deposition of microbial cell walls that make up the calculus. The calculus adjacent to the cementum is densely packed, interconnected, and fused, making the calculus–cementum interface indistinguishable (Tan et al., 2004).

Compared to SCMG 0665 (Fig. 3) the extant *Pontoporia blainvillei* tooth (Figs. 11A, 11B) has an indistinguishable CEJ and a shiny surface without any visible accretions. Its lateral view shows a smooth bulge on the right side of the image (anterior side), without a corresponding bulge on the left side. The anterior view reveals a slight thickening on the root surface. In contrast, the fossil allodelphinid plantanistoid tooth (Figs. 11C, 11D) has a complete crown and most of the root has a uniform surface with a gentle thickening of the crown toward the CEJ. The root surface below the CEJ is the thickest part of the tooth, with a swelling on the anterior aspect. The lateral and anterior views of the fossil tooth reveal a slight mineral deposit (Fig. 11, arrows).

DISCUSSION

The calculus-like deposit found on the root surface of the tooth from SCMG 0665 suggests that there was localized periodontal disease in at least one alveolus. Bone loss, an indication of periodontal disease, is assumed if the calculus forms on the root surface (Figs. 1, 3, 4; Cobb, 2008; Carranza and Newman, 1995; Page and Schroeder, 1982).

The bulge on SCMG 0665 is similar in form to a supragingival calculus deposit that would accumulate at or just above the gingival line (Figs. 3, 4A; Gurenlian, 2007; Hillson, 2005; Lustmann et al., 1976). On the root side of the bulge, the mineral deposits are similar to subgingival calculus in their compact structure, (Figs. 1, 3, 4–6). Images of the extant dolphin tooth (LACM 47143 *Pontoporia blainvillei* Figs. 11A, 11B) and the fossil odontocete tooth specimen (LACM 123887; Fig. 11C, 11D) were compared with SCMG 0665 (Fig. 3). The extant *Pontoporia blainvillei*) tooth has a shiny surface with a smooth bulge that appears to be normal anatomy, and has no visible accretions. The fossil odontocete tooth has a distinguishable

crown, CEJ, and swollen root surface with a small mineral deposit. Swollen roots of teeth have been considered diagnostic in some fossil and extant Odontoceti but such diagnosis is based on normal anatomy, not on mineral deposits, accretions, or pathology. The swollen root on SCMG 0665 is a mineral deposit.

The SEM image (Fig. 7B) illustrates the compact structure of the mineral deposit near the tooth surface and the irregular layers near its top, both of which are characteristic of calculus (Figs. 2A, 2B; Rohanizadeh and LeGeros, 2004). Fractures seen in Figures 4, 7A, and 9 appear, as in human calculus, to be within the deposit—thereby further supporting our interpretation. The fractures in the calculus of SCMG 0665 are consistent with the findings of Abraham et al. (2007), Rohanizadeh and LeGeros (2004), Carranza and Newman (1995), and Lustmann et al. (1976) that fractures occur within the calculus matrix, not at the calculus–cementum interface.

The root surface on the tooth from SCMG 0665 has a rough and irregular surface with varied colors (Figs. 4, 5A, 6, 7). The composition of the fossilized calculus-like deposit on SCMG 0665 is calcium phosphate ($Ca_{10}(PO_4)_6$, Fig. 8; Table 1), which is similar to the composition of enamel, dentin, cementum, and dental calculus (Avery and Chiego, 2006). Ameloblasts, odontoblasts, and cementoblasts arrange tissue matrix in uniform layers (Figs. 1B, 5F; Avery and Chiego, 2006; Brand and Isselhard, 1990), whereas calculus is formed by bacteria in dental plaque (biofilm) and the initial deposition is irregular and heterogeneous (Cobb, 2008; Tan et al., 2004; Carranza and Newman, 1995).

Microbial tubules cover the root surface, the wall of the chipped deposit, and the outer covering of the root surface (Figs. 4C, 5B, 7) but none were seen on enamel. Microbial tubules within the matrix of the deposit and embedded in the deposit on the root surface display characteristics of dental calculus (Figs. 4–7, 9; Wilkins, 2009; Cobb, 2008; Tan et al., 2004; Carranza and Newman, 1995). The calculus and microbial tubules of SCMG 0665 (Figs. 6A, 6B) present a marked similarity to human calculus (Figs. 2C, 2D). The microscopic tubules in Figures 2C and 2D are 4–7 μm wide, consistent with eukaryotic filamentous fungi or algae (Prescott et al., 1990). The presence of the microtubules indicates the bulge of the calculus-like structure around the tooth is not an abiotic concretion.

CONCLUSION

The mineral deposit found on a fossil odontocete tooth from a partial skull collected from the late Miocene Monterey Formation at Horse Beach Canyon on San Clemente Island, Los Angeles County, California, USA, is consistent with dental calculus. The deposit—rough and irregular on its surface—is similar in morphology to calculus on both extant and fossil mammal teeth. Interpretation of the deposit as calculus is further supported by the presence of a fracture within the calculus. The presence of calculus deposit on the root surface indicates that there was localized periodontal disease in at least one alveolus and perhaps others. Periodontal disease has been documented in seven extant odontocete cetaceans, but this is believed to be the first documentation of dental calculus and periodontal disease in a fossil odontocete.

ACKNOWLEDGMENTS

We convey many thanks to Lawrence G. Barnes, LACM, for encouraging this research, and for sharing his knowledge and resources. David B. Jones and the David B. Jones Foundation provided funding for this research, as well as encouragement and enthusiastic support. We thank William K. Matteson from Sheridan College Museum of Discovery and Howell W. Thomas of LACM for preparation of the specimen. Jeb A. Taylor and Brian X. Flynn provided photographs of the specimen. Vanessa R. Rhue (LACM) helped with photos of SCMG 0665 and made photos of the *Pontoporia blainvillei* tooth; James Dines, Collections Manager for LACM Department of Mammalogy gave permission to study it. Edward F. Duke (Engineering and Mining Experiment Station [EMES], South Dakota School of Mines and Technology [SDSMT]) provided access to SEM. Charles M. Cobb, University of Missouri at Kansas City, was very generous with his time and expertise in interpreting dental calculus and periodontal disease in our SEM images and for providing unpublished SEM images of human calculus. Bruce M. Rothschild of the University of Kansas Museum of Natural History and the Carnegie Museum was very helpful with expertise in paleopathology. Jan K. Larson, (Environmental Department of the Navy, Region Southwest) was generous with his time, granted the research permit (Cooperative Research Agreement 04-01), and facilitated our trips to San Clemente Island, California. We thank Wilfred J. Sturgeon and Michael J. Flynn, whose correspondence initiated the trip to San Clemente Island, and consequently, this research.

LITERATURE CITED

Abraham, J.A., M.S. Grenon, H.J. Sanchez, M.C. Valentinuzzi, and C.A. Perez. 2007. μX-ray fluorescence analysis of traces and calcium phosphate phases on tooth–tartar interfaces using synchrotron radiation. *Spectrochimica Acta, Part B* 62:689–694.

American Academy of Periodontology. 2011. Types of gum disease. http://www.perio.org/consumer/2a.html.

Avery, J.K., and D.J. Chiego. 2006. *Essentials of oral histology and embryology*: *A clinical approach*, Third ed. Mosby - Year Book, Inc., St. Louis, MO, 241 pp.

Bjotvedt, G., and C.G. Turner, II. 1977. Mandibular lesions of prehistoric Aleutian sea mammals. *Journal of Wildlife Diseases* 13:360–365.

Brand, R.W., and D.E. Isselhard. 1990. *Anatomy of Orofacial structures*, Fourth ed. The C.V. Mosby Company, St. Louis, MO, 496 pp.

Carranza, F.A., and M.G. Newman. 1995. *Glickman's clinical periodontology*, 8th ed. Philadelphia, Pennsylvania: W.B. Saunders Company, 840.

Cobb, C.M. 2008. Microbes, inflammation, scaling and root planing, and the periodontal condition. *Journal of Dental Hygiene* 83(6):4–9.

Craig, R.G., P. Kotanko, A.R. Kamer, and N.W. Levin. 2007. Periodontal diseases—A modifiable source of systemic inflammation for the end-stage renal disease patient on hemodialysis therapy? *Oxford Journals, Nephrology Dialysis Transplantation* 22:312–315.

Dobney, K., and D. Brothwell. 1986. A method for evaluating the amount of dental calculus on teeth from archaeological sites. *Journal of Archaeological Science* 14:343–351.

———. 1988. A scanning electron microscopy study of archaeological dental calculus. In *Scanning Electron Microscopy in Archaeology*, ed. S. Olsen. Oxford, BAR International Series 452:372–385.

Forsberg, A., C. Lagergen, and T. Lonnerblad. 1960. Dental calculus: Biophysical study. *Oral Surgery, Oral Medicine, Oral Pathology* 13(9):1051–1060.

Gerholdt, J.M., and S.J. Godfrey. 2010. Enigmatic osteology in Miocene Odontocete rostra suggests periostitis. *Marine Mammal Science* 26(2):381–394.

Gurenlian, J.R. 2007. The role of dental plaque biofilm in oral health. *Journal of Dental Hygiene* Special Supplement, 4–12.

Hart Hansen, J.P., J. Meldgaard, and J. Nordqvist (eds). 1991. *The Greenland mummies*. Washington, D.C.: Smithsonian Institution Press, 192 pp.

Hillson, S. 2005. *Teeth*, 2nd ed. New York: Cambridge University Press, 373.

Lustmann, J., J. Lewin-Epstein, and A. Shteyer. 1976. Scanning electron microscopy of dental calculus. *Calcified Tissue International* 21(12):47–55.

Moodie, R.L. 1923. *Paleopathology. An introduction to the study of ancient evidences of disease*. Urbana: University of Illinois Press, 567 pp.

Myrick, A.C., A.A. Hohn, P.A. Sloan, M. Kimura, and D.D. Stanley. 1983. Estimating age of spotted and spinner dolphins (*Stenella attenuata* and *Stenella longirostris*) from teeth. NOAA Technical Memorandum NMFS, NOAA/ National Marine Fisheries Service/ Southwest Fisheries Science Center, SWFC-30:1–23.

Overman, P.R. 2006. Biofilm: A new view of plaque. *The Journal of Contemporary Dental Practice* 1(3):1–11.
Page, R.C., and H.E. Schroeder. 1982. *Periodontitis in man and other animals, a comparative review*. New York: Karger, 330 pp.
Perrin, W. 2010. World Cetacea Database. http://www.marinespecies.org/cetacea/aphia.php?p=taxdetails&id=137093.
Prescott, L.M., J.P. Harley, and D.A. Klein. 1990. *Microbiology*. Dubuque, IA: Wm. C. Brown Publishers, 882 pp.
Rothschild, B.M., and L.D. Martin. 1993. *Paleopathology: Disease in the fossil record*. Boca Raton, FL: CRC Press, Inc., 386 pp.
———. 2006. *Skeletal Impact of Disease*. Albuquerque, NM: New Mexico Museum of Natural History and Science, Bulletin 33, 226 pp.
Rohanizadeh, R., and R.Z. LeGeros. 2004. Ulrastructural study of calculus–enamel and calculus–root interfaces. *Archives of Oral Biology* 50:89–96.
Socransky, S.S. 1970. Relationship of bacteria to the etiology of periodontal disease. *Journal of Dental Research* 49:203–222.
Socransky, S.S., and A.D. Haffajee. 2005. Periodontal microbial ecology. *Periodontology 2000* 38:135–187.
Tan, B., D.G. Gilliam, N.J. Mordan, and P.N. Galgut. 2004. A preliminary investigation into the ultrastructure of dental calculus and associated bacteria. *Journal of Clinical Periodontology* 31:364–369.
Van Bressem, M., K. Van Waerebeek, D. Montes, S. Kennedy, J.C. Reyes, I.A. Garcia-Godos, K. Onton-Silva, and J. Alfaro-Shigueto. 2006. Diseases, lesions and malformations in the long-beaked common dolphin (*Delphinus capensis*) from the Southeast Pacific. *Diseases of Aquatic Organisms* 68:149–165.
Van Bressem, M., J.C. Van Waerebeek, F. Reyes, M. Felix, S. Echegaray, A. P Siciliano, L. Di Beneditto, F. Flach, I.C. Viddi, J.C. Avila, I.C. Herrera, J. Tobon, I.B. Bolanos, P.H. Moreno, G.P. Ott, E. Sanino, D. Castineira, E. Montes, P.A.C. Crespo, B. Flores, S.M.F. Haase, M. Mendonca de Souza, A.B. Fragoso, and L. Fragoso. 2007. A preliminary overview of skin and skeletal diseases and traumata in small cetaceans from South American waters. *Latin Journal of Aquatic Mammals* 6(2007):7–42.
Wilkins, E.M. 2009. *Clinical Practice of the Dental Hygienist,* 10th ed. Philadelphia, Pennsylvania: Lippincott Williams and Wilkins, 1197 pp.

Received 30 May 2011; accepted 29 November 2012.

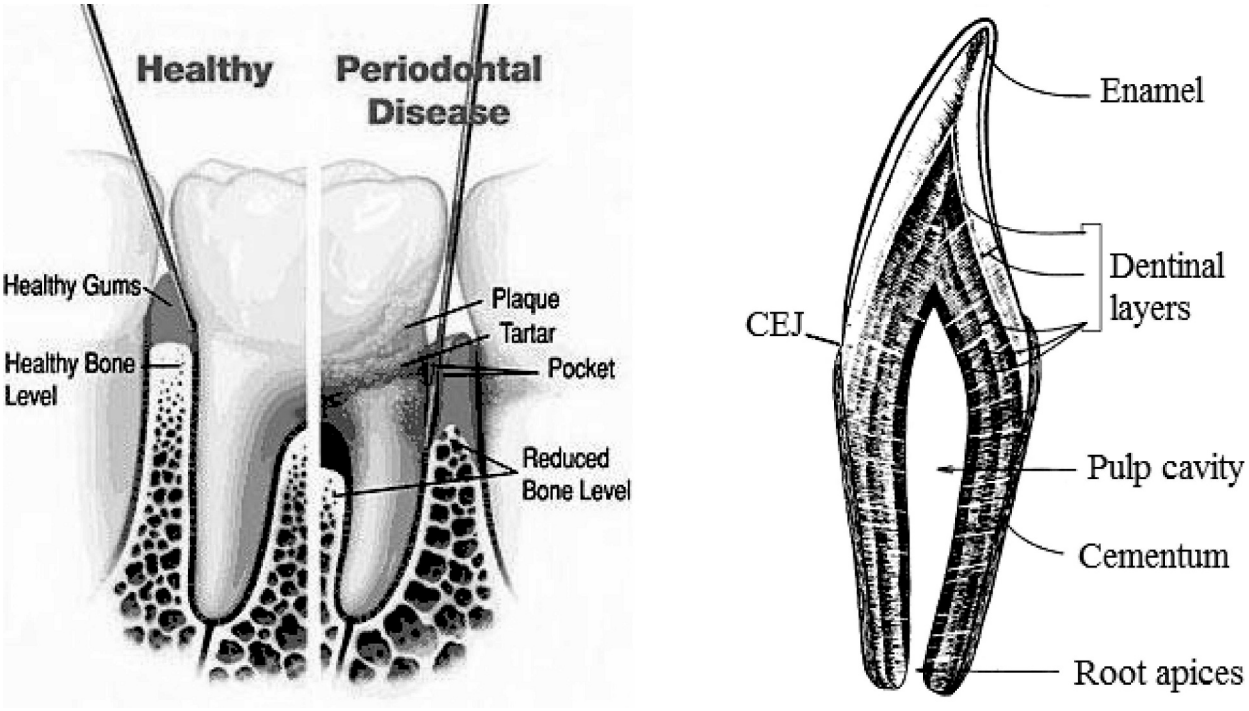

Figure 1 Left, An illustration of the difference between healthy bone and gingival tissues and the destruction of the periodontium due to periodontal disease (pyorrhea). Note the loss of bone, the increased porosity of that bone, the detachment of the gingiva, and loss of periodontal ligaments, causing a pocket. Note the position of the plaque and calculus (tartar) at and just below the gingival line, as well as the darker calculus more apical (toward the root tip) on the root surface (American Academy of Periodontology, 2011). **Right,** Diagram of a dolphin tooth in longitudinal section displaying tissues and structural anatomy, adapted from Myrick et al. (1983).

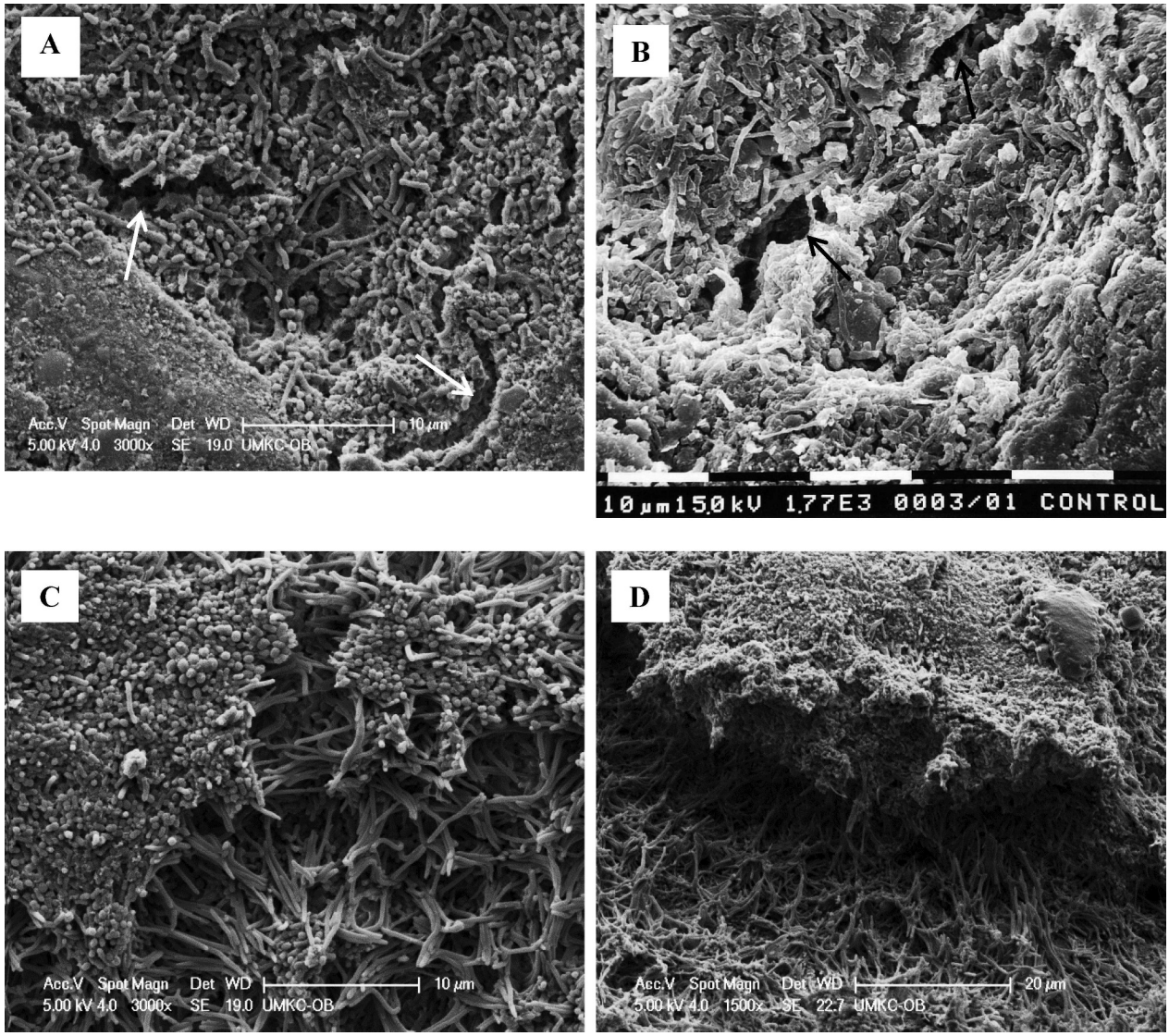

Figure 2 SEM images of human calculus, all having a thick layer of surface biofilm; **A** and **B,** note fractures within the calculus images (arrows) and, **C** and **D,** pattern of adherent filamentous bacteria. SEMs (unpublished) courtesy of Charles M. Cobb, University of Missouri at Kansas City.

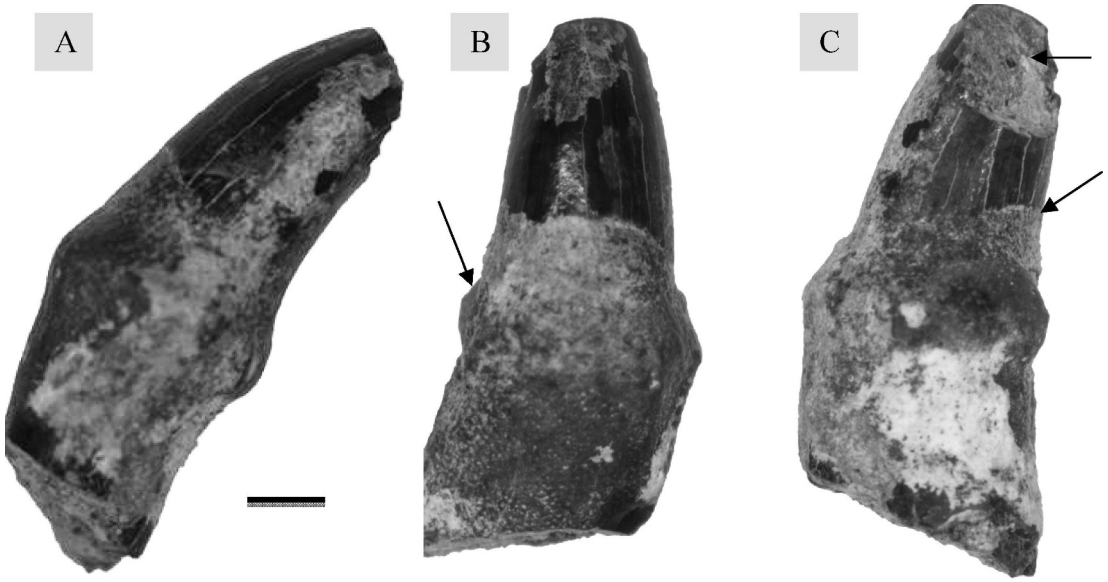

Figure 3 Odontoceti, genus and species undetermined, tooth associated with skull SCMG 0665, late Miocene, Monterey Formation, San Clemente Island, Los Angeles County, California; **A**, anterior view, bulge is proximal to the CEJ, unidentified light-colored deposit follows the longitudinal axis of the tooth; **B**, buccal view showing shiny enamel crown, arrow points to chip exposing portion of the mineral deposit, and darker underlying surface of the root, mineral deposit on the lower left portion of the root surface has a stippled texture; **C**, lingual view, upper arrow indicates pulp canal in crown, lower arrow points to CEJ; actual size is 8.9 mm long × 4.3 mm in diameter; scale bar = 1 mm.

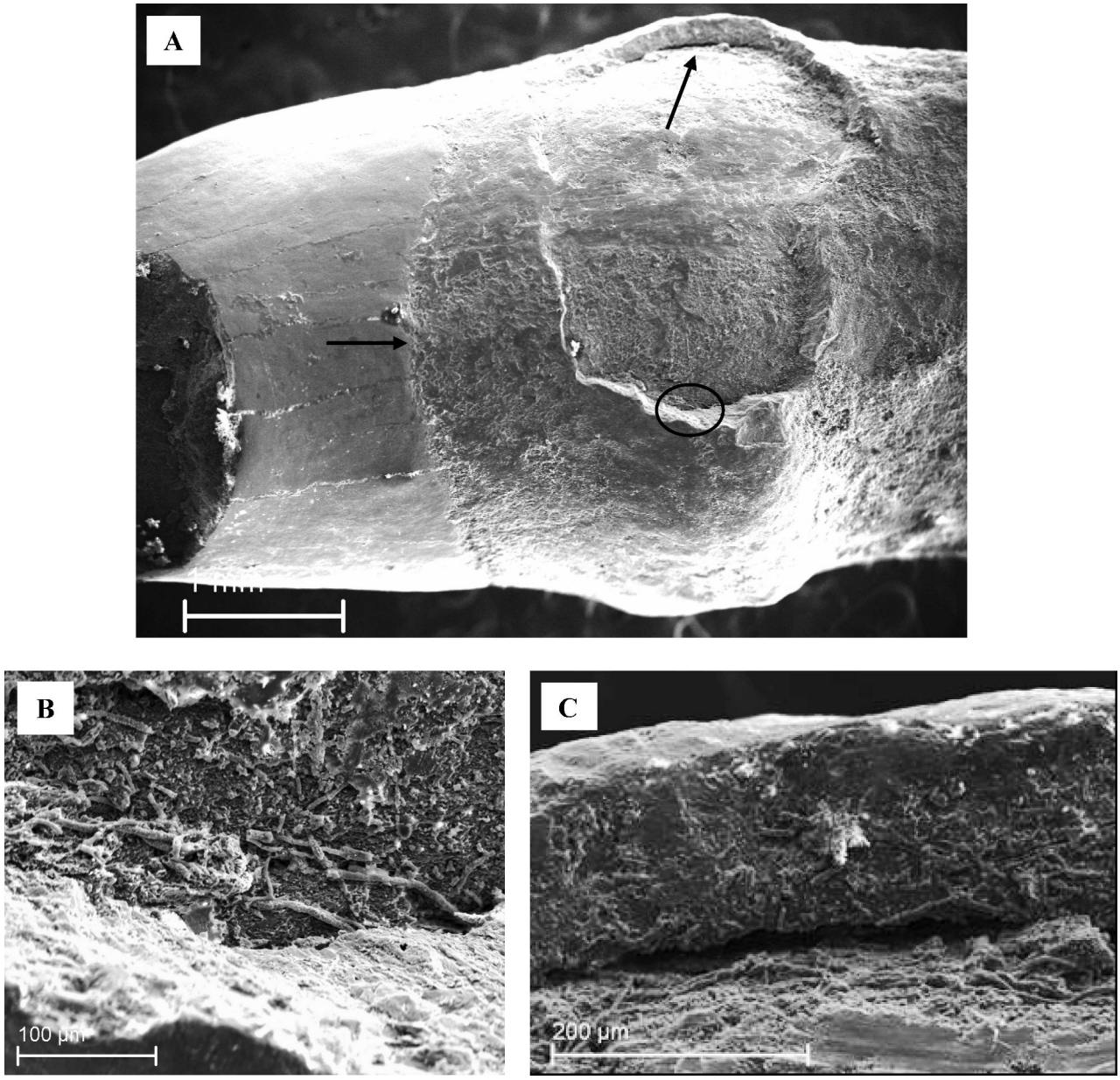

Figure 4 Odontoceti, genus and species undetermined, SEM images of tooth associated with skull SCMG 0665, late Miocene, Monterey Formation, San Clemente Island, Los Angeles County, California; **A,** posterior surface of root showing broken area in surface deposit with fracture in this material indicated by upper arrow, lower arrow indicates CEJ, oval indicates area in B; **B,** enlargement of broken area indicated by the oval in A; **C,** enlargement of fracture between surface deposit and tooth root that is seen in A.

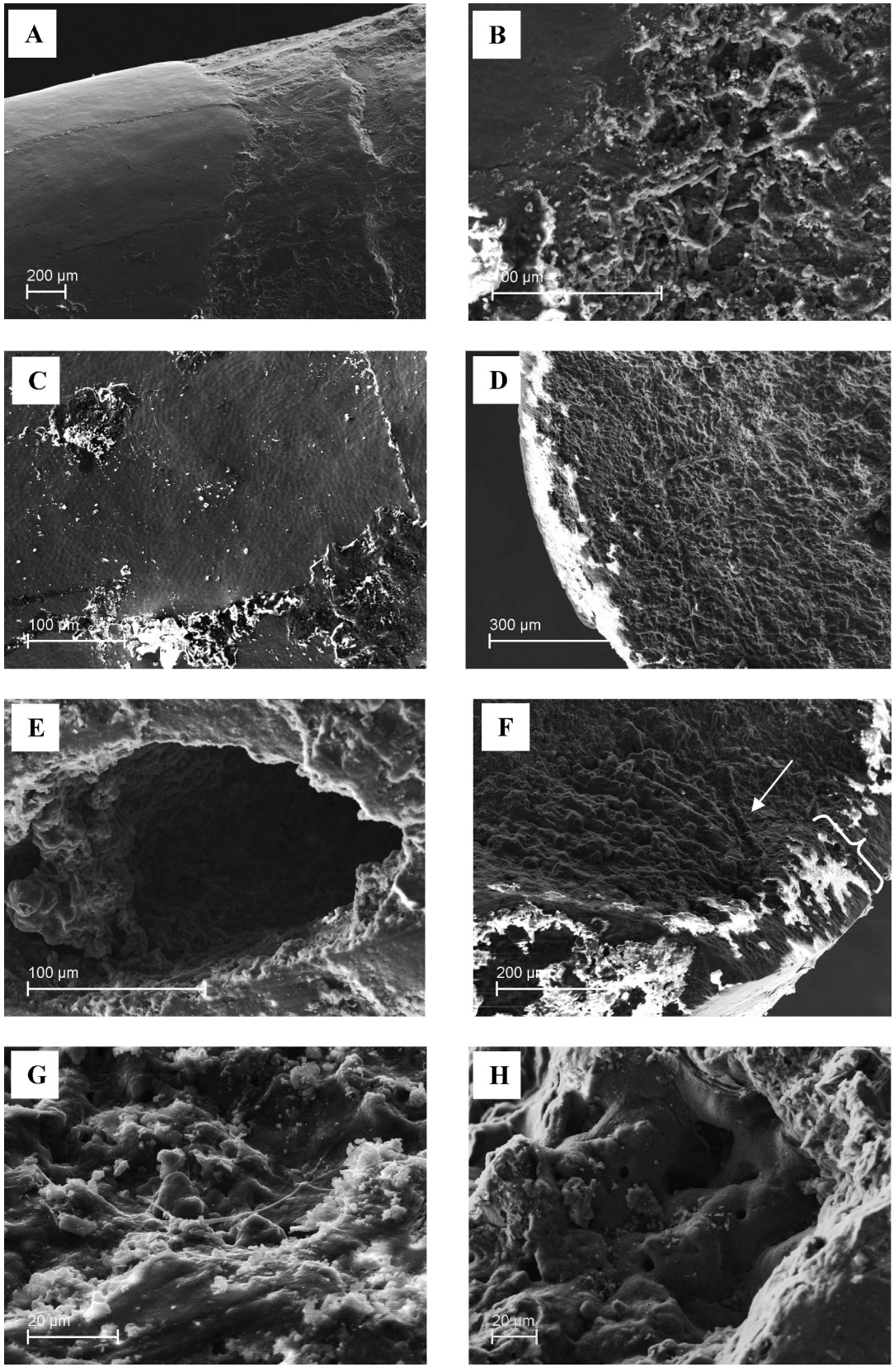
A
200 µm
B
100 µm
C
100 µm
D
300 µm
E
100 µm
F
200 µm
G
20 µm
H
20 µm

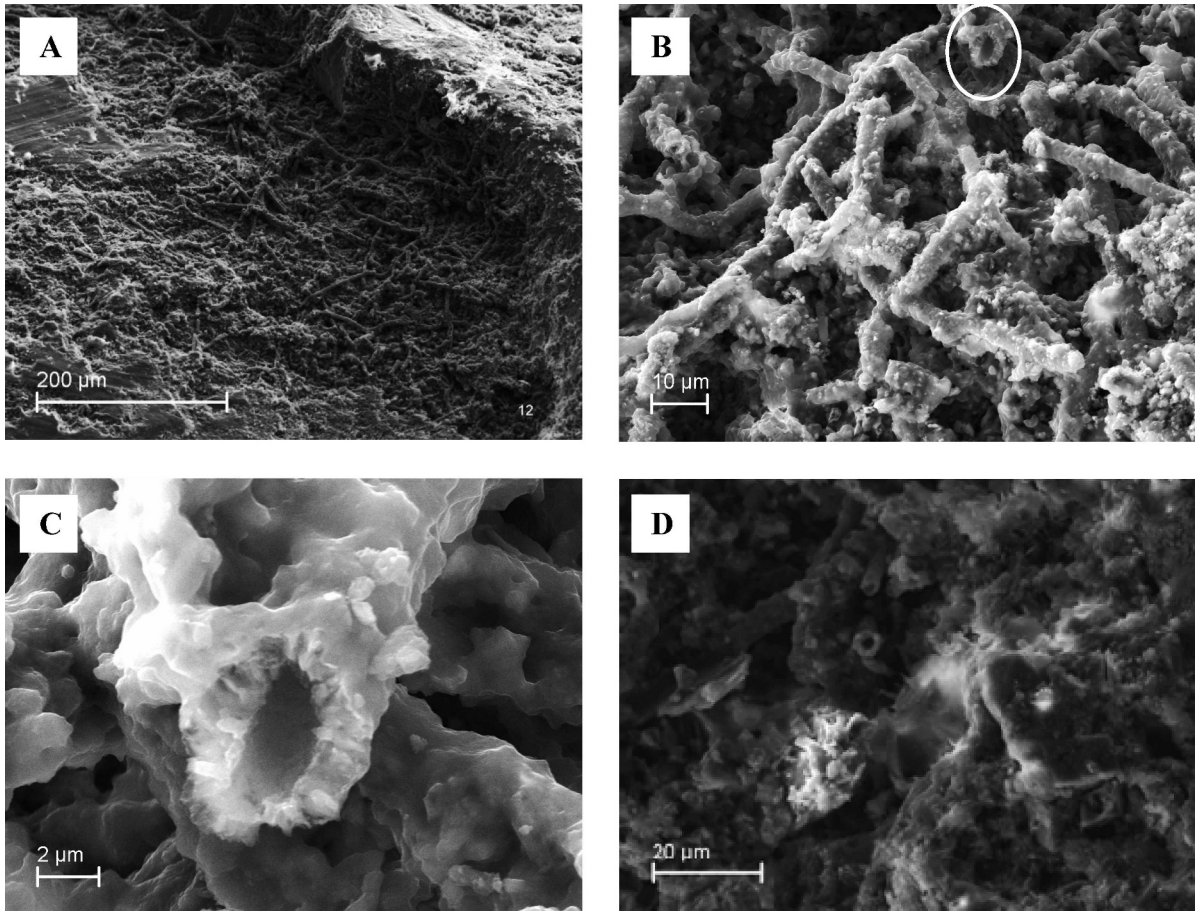

Figure 6 Odontoceti, genus and species undetermined, SEM images of tooth associated with skull SCMG 0665; **A,** thick mat of adherent microbial tubules in the fracture of the mineral deposit; **B,** filamental microbial tubules; **C,** enlargement of a hyphal lumen in image B (oval); **D,** filamental microbial tubules in matrix of the mineral deposit on the root surface.

←

Figure 5 Odontoceti, genus and species undetermined, SEM images of tooth associated with skull SCMG 0665; **A,** CEJ, note the smooth, dense surface of the enamel on the left compared to the rough, irregular, fractured root surface on the right; **B,** filamental microbial tubules at the CEJ embedded in the root surface (calculocementum); **C,** dimpled surface of the enamel; **D,** surface of the broken crown with a partial view of the pulp canal on the right side of the image; **E,** enlargement of the pulp canal; **F,** dentoenamel junction, note the enamel rods (bracket) interfacing the globular dentin and filamental tubules (arrow); **G,** root surface with pores and filaments; **H,** root surface is uneven with pores, may be dentinal tubules or anchors for periodontal ligaments.

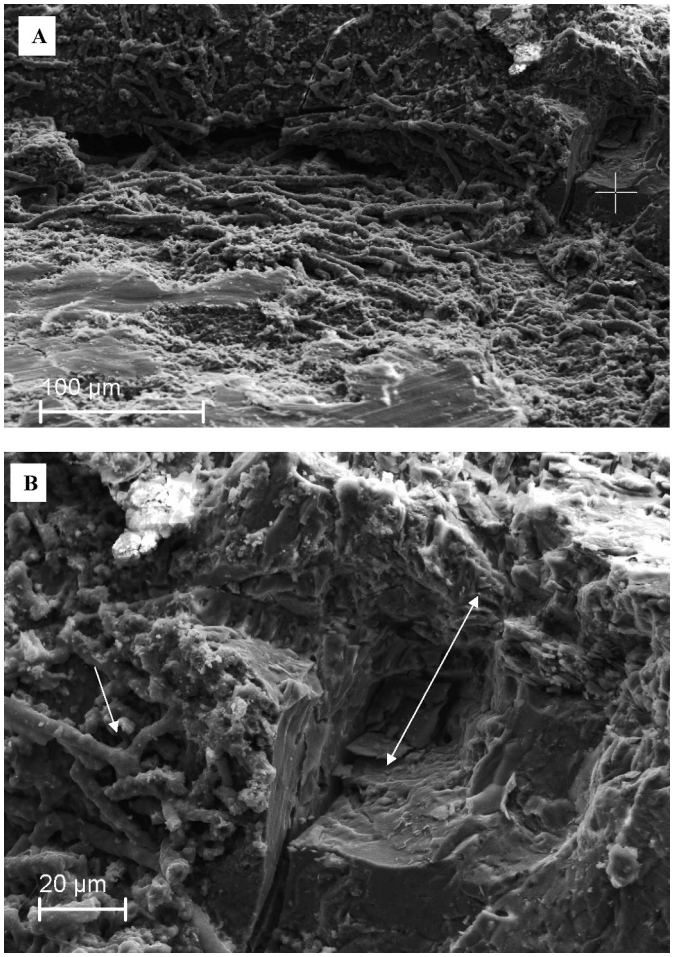

Figure 7 Odontoceti, genus and species undetermined, SEM images of tooth associated with skull SCMG 0665; **A**, cross-hair marker corresponds to EDX analysis in Figure 8 and Table 1, note microbial tubules; **B**, increased magnification of area analyzed in A, note the compact structure of the mineral deposit on the bottom and the irregular structure of the deposit near and at the top (double arrow), note branching tubules of calcium carbonate (small arrow).

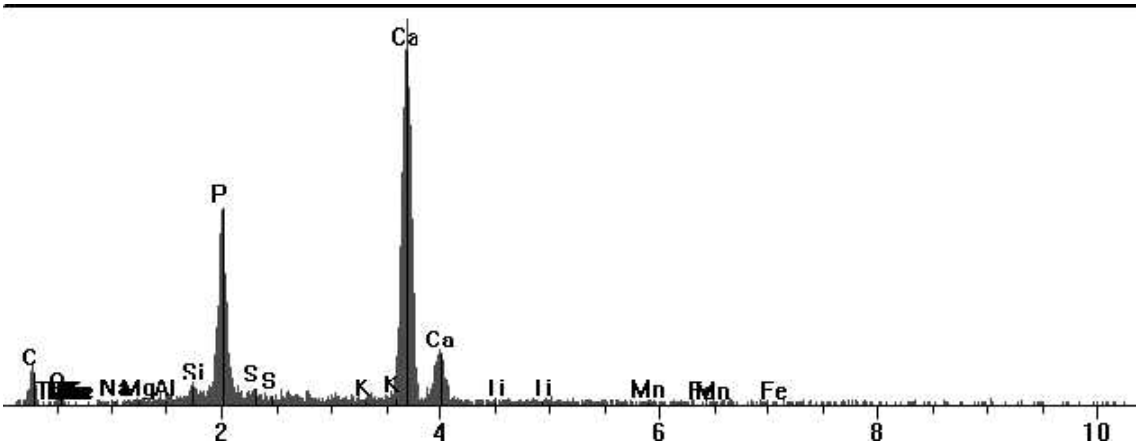

Figure 8 Graph from EDX spectrum report on the mineral deposit of SCMG 0665 (Fig. 7); elemental composition that is consistent with calcium phosphate (hydroxyapatite).

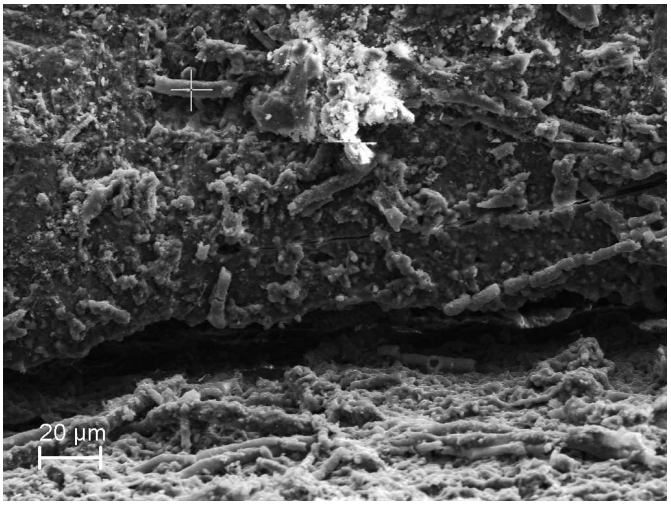

Figure 9 Odontoceti, genus and species undetermined, SEM image of tooth associated with skull SCMG 0665; marker on microbial tubule indicates the site of the EDX analysis in Figure 10 and Table 2. The marked tubule measures approximately 7 µm wide and 22 µm long. As a comparison, a bacterium found in a human oral cavity, *Actinomycetes*, that forms hyphae can measure 20 µm and longer with a width of 0.5–2.0µm (Prescott et al., 1990).

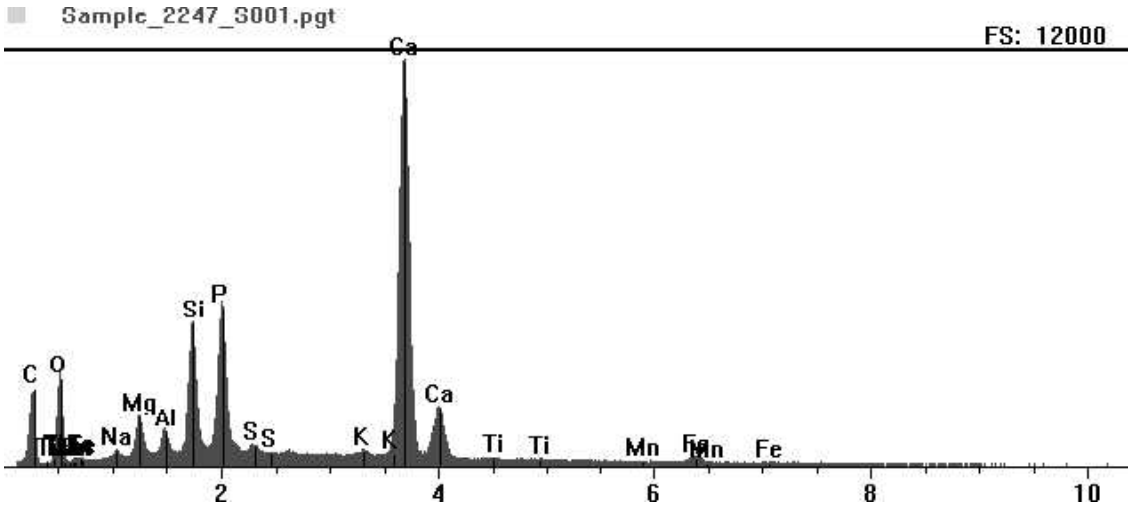

Figure 10 Graph from EDX spectrum report for the area analyzed (Fig. 9), indicated by a cross mark on the microbial tubule. Elemental composition is consistent with calcium carbonate.

Figure 11 Extant dolphin tooth and fossil dolphin tooth (used with permission) presented for comparison with SCMG 0665. **Top:** Extant dolphin tooth image of LACM 47143 *Pontoporia blainvillei* (Gervais and d'Orbigny, 1844), **A,** lateral view; note the bulge on the right side of the image (facial side) without a corresponding bulge on the left side of the image, note indistinguishable CEJ; **B,** facial view reveals a slight thickening on the root surface, which appears to be normal anatomy of this specimen. **Bottom:** fossil Odontocete tooth (LACM 123887 unnamed species of allodelphinid plantanistoid odontocete); **C,** lateral view displays a slight bulge on the left side or (facial side); **D,** the facial view does not show any bulge near the CEJ, note the faint mineral deposit on root surface (arrows).